

The photocatalytic reduction of NO_3^- to N_2 with ilmenite (FeTiO_3): Effects of groundwater matrix

Jefferson E. Silveira^{a,*}, Alyson R. Ribeiro^{a,b}, Jaime Carbajo^a, Gema Pliego^a, Juan A. Zazo^a, Jose A. Casas^a

^a Department of Chemical Engineering, Universidad Autónoma de Madrid, Madrid 28049, Spain

^b Department of Analytical Chemistry, Institute of Chemistry, University of Campinas, P.O. Box 6154, Campinas, SP 13084-971, Brazil

ARTICLE INFO

Article history:

Received 20 October 2020

Revised 2 May 2021

Accepted 10 May 2021

Available online 15 May 2021

Keywords:

Nitrate

Photo-reduction

Groundwater

Ilmenite

Water conditioning

ABSTRACT

This work analyzes the role of natural groundwater, as well as the effect of HCO_3^- , Ca^{2+} , Mg^{2+} , K^+ , SO_4^{2-} and Cl^- concentrations, upon the photocatalytic nitrate reduction using ilmenite as catalyst and oxalic acid as hole scavenger. The nitrate removal and the selectivity towards N_2 are significantly limited compared to previous experiments using ultrapure water matrix. Calcium (Ca^{2+}), bicarbonate (HCO_3^-) as well as pH are claimed as the major controlling factors related to the process yield. Thus, Ca^{2+} promotes the formation of insoluble oxalate microcrystals, reducing the amount of hole scavenger available. The presence of HCO_3^- leads to a steeply increase in the pH value, favoring the adsorption onto the ilmenite surface of ions OH^- instead of NO_3^- , NO_2^- and $\text{C}_2\text{O}_4^{2-}$. The aforementioned issues are overcome by working with $\text{C}_2\text{O}_4^{2-}/\text{NO}_3^-$ ratio well above the stoichiometric one, that also maintains the pH value in an acid range. A completed depletion of the starting NO_3^- , the no detection of either NO_2^- or NH_4^+ in the aqueous phase, and a selectivity towards N_2 above 95% were achieved using two times the stoichiometric dose.

© 2021 The Author(s). Published by Elsevier Ltd.

This is an open access article under the CC BY-NC-ND license (<http://creativecommons.org/licenses/by-nc-nd/4.0/>)

1. Introduction

Nitrate is one of the main pollutants of groundwater in Europe and USA and has affected several regions worldwide (Biddau et al., 2017; Krempa and Flickinger, 2017;). Vital for plants and crops growth, the excess of this nutrient reach water bodies by run-off and leaching of manure and fertilizers applied in agricultural areas as well as from improper disposal of livestock and fish farms effluents. For instance, from 2012 to 2014, 9.2 ktonnes of animal manure nitrogen were used by the 27 EU Member States and UK for agricultural activities. Moreover, in those states, both the use and the amounts used of manure and mineral fertilizer nitrogen were remarkably similar (SWD, 2018). According to the receiving soil characteristics as redox potential, permeability and denitrification capacity, nitrate percolates and can accumulate in groundwater (Biddau et al., 2017). Sewage and its sludge also contribute to the release of nitrogen compounds into the aquatic matrices in urbanized regions, leading to recurrent algal blooms issues and com-

promised water drinkability (EU, 2006). The control of diffuse pollution sources is challenging and rises concern over nitrate public health consequences, as the blue baby syndrome and gastrointestinal disorders (Karanasios et al., 2010; Pennino et al., 2017). For sensitive aquatic organism's protection, Camargo et al. (2005) indicate 2 mg N/L as the upper limit concentration of nitrate.

Legal actions across Europe and North America, among other areas, have been taken to protect human health and the aquatic ecosystems balance (Krempa and Flickinger, 2017; SWD, 2018). To illustrate, codes of good agricultural practice were adopted in the EU-27 and UK level as well as Nitrate Vulnerable Zones (NVZ) were established. However, a recent European Commission report exposed that average annual nitrate concentration was equal to or exceeded the threshold of 50 mg/L (EU, 2006; WHO, 2011) in several fresh and saline surface water and groundwater monitoring stations during the reporting period 2012–2015 (SWD, 2018). Whereas an overall decreasing trend in average nitrate concentrations was observed, for some countries as Spain, Malta and Germany, the number of monitored station showing exceeded concentrations in groundwater was higher than 21% (SWD, 2018; COM, 2018).

* Corresponding author.

E-mail address: jefferson.silveira@uam.es (J.E. Silveira).

Table 1
Physico-chemical properties of ilmenite.

FeTiO ₃ /TiO ₂ phases (%)	S _{BET} (m ² g ⁻¹)	Fe(III)/Fe(II) (surface)	Fe/Ti weight (%)	Band-gap value (eV)
85/15	6	58/42	36/37	2.4

As a representative example, Lastras de Cuéllar, Spain, as well as other municipalities in the Duero River basin have faced serious drinking water supply issues due to unacceptable levels of agricultural nitrate. Located in the Iberian Peninsula biggest aquifers system, this basin population toggles between arsenic and nitrate groundwater contamination, resulting in recurrent water supply cessation (García-Costa et al., 2020; Mayorga et al., 2013). The available technologies to deal with this problem at the industrial scale are based on separation processes, mostly ion exchange and reverse osmosis but also electrodialysis (Jensen et al., 2014). The main common drawback to separation technologies is the generation of a residual brine in which nitrates are concentrated that must be properly disposed. The high capital and operational costs are also significant for reverse osmosis. Biological denitrification has been also postulated as an alternative (Liu et al., 2020). However, it requires a further stage to remove the denitrifying bacteria and the remaining nutrients.

Catalytic hydrogenation has been considered as a promising alternative to overcome the economic and ecological disadvantages of separation technologies, as NO₃⁻ is ideally converted to N₂ without generating waste streams (Ruiz-Beviá and Fernández-Torres, 2019). The main challenge, still unsolved, focuses on accomplish a suitable catalyst able to selectively reduce nitrates towards N₂ avoiding the occurrence of other toxic nitrogenous byproducts (NO₂⁻ and NH₄⁺) that ultimate prevent water use for human consumption.

Photocatalytic reduction is currently the most favorable alternative to separation technologies for a further implementation on an industrial scale. This treatment is based on the photo-excitation of a semiconductor (usually TiO₂ or materials based on TiO₂) generating an e_{bc}⁻/h_{bv}⁺ pair. The e_{bc}⁻ reduce the NO₃⁻ adsorbed on the surface of the photocatalyst. Besides, another specie (i.e. hole scavenger) is necessary to provide electrons to fill in h_{bv}⁺ and closure the redox cycle.

Materials based on metal oxides, sulfides, perovskites among others have been used as photocatalysts to enhance nitrate removal from aqueous solution. Among this variety, it is worth to mention the recent works using enhanced structures, as aluminium oxide-based nanocomposites (Velu et al., 2021), the non-linear optical material lithium niobate (Li et al., 2021) and poly-oxometalates (Wang et al., 2021). However, the disadvantages of those catalysts as complex synthetization and characterization as well as their high cost need to be considered and overcome.

In that direction, the natural mineral ilmenite (FeTiO₃) has been suggested as a low-cost photo-catalyst. This titanate-based antiferromagnetic semiconductor presents a band gap ranging from 2.4 to 2.9 eV and showed significant stability and effectiveness when used as a catalyst in different advanced oxidation processes (García-Muñoz et al., 2016; Silveira et al., 2017; Zazo et al., 2020). Recently, our research group presented the promising use of FeTiO₃ and oxalic acid, as reducing agent, for the selective photo-reduction of nitrate to N₂ (Zazo et al., 2020). Using ultrapure water, this process showed high selective towards N₂, the complete removal of NO₃⁻ and C₂O₄²⁻ and almost negligible formation of NO_x (g). Therefore, there is a potential interest of using the FeTiO₃ and oxalic acid photocatalytic method for the treatment and/or polishing of natural waters containing nitrate. However, it is worth to highlight that during natural water treatment the presence of species in solution that react competitively with h_{bv}⁺, e_{cb}⁻ over

photocatalyst or the redox mediators may significantly affect the efficiency due to adsorption onto the catalytic surface. These photosensitizer species occur naturally in water, can be left over conventional water processing and will, in most cases, decrease the reaction velocity of photocatalytic polishing steps (Yang et al., 2013). The total nitrate reduction suppression has been reported due to the presence of high concentration of CO₃²⁻ which can poison the photocatalyst. Similarly, sulfates can aggregate onto nanoparticles of TiO₂, reducing its exposed surface and the overall catalytic efficiency (Zhang et al., 2005). Therefore, the selectivity to nitrogen and the effects of water matrix are important factors that should be assessed for any proposed technology for nitrate removal.

In this work we investigated the photocatalytic nitrate removal process using ilmenite and oxalic acid as hole scavenger as a polishing step of natural groundwater as well as the effect of concentrations of photosensitizer and ions as HCO₃⁻, Ca²⁺, Mg²⁺, K⁺, SO₄²⁻ and Cl⁻, in the treatment efficiency. To bring a more realistic scenario, aqueous samples of raw and filtered Duero basin groundwater, a critical contaminated region, were also employed.

2. Material and methods

2.1. Chemicals and reactants

The NaNO₃ (≥ 99% purity) used for nitrate aqueous solution preparation, the oxalic acid dihydrate (≥ 99% purity) as well as all other chemicals used were purchased from Sigma-Aldrich, USA. N₂ (g) (L50) was supplied by Praxair S.L. The ilmenite (Ref. 50,110,700) was provided by Marphil S.L. (Spain). Table 1 summarizes the main physico-chemical properties of the used ilmenite. Further characterization parameters from the employed ilmenite are available elsewhere (Silveira et al., 2017; Zazo et al., 2020).

2.2. Environmental sampling and matrices composition

Groundwater samples were collected at Lastras de Cuéllar (Segovia, Spain) in February 2020 before (RW) and after (TW) passed through an iron oxide-hydroxide filter (Bayoxide E-33) to retain arsenic. After arrival at the lab, the samples were immediately analyzed for pH, carbon content, nitrate, chloride, sulfate and calcium (Table 2), stabilized under refrigeration (4 °C) and used within 5 days. Additionally, ultrapure water obtained from Millipore milli-Q system was used as solvent to prepare sole solutions of the main water matrix constituents HCO₃⁻ (160), Ca²⁺ (60), Mg²⁺ (20), K⁺ (10), SO₄²⁻ (90) and Cl⁻ (80), at fixed concentrations, in mg/L.

2.3. Photocatalytic experiments

The system consisted of a sealed glass jacketed batch reactor placed on top of a magnetic stirrer, with reaction volume set at 750 mL. A 150 W commercial medium pressure mercury lamp (TQ150 Heraeus, Germany), 30 W cm⁻², was placed at the center of the cylindrical reactor (Fig. S1).

The incident UV-Vis irradiation has been directly measured by a broad range photoradiometer (Delta Ohm, model HD 2102.1). In addition, the emission spectrum distribution given by the manufacturer is provided in the Supporting Information (Fig. S2).

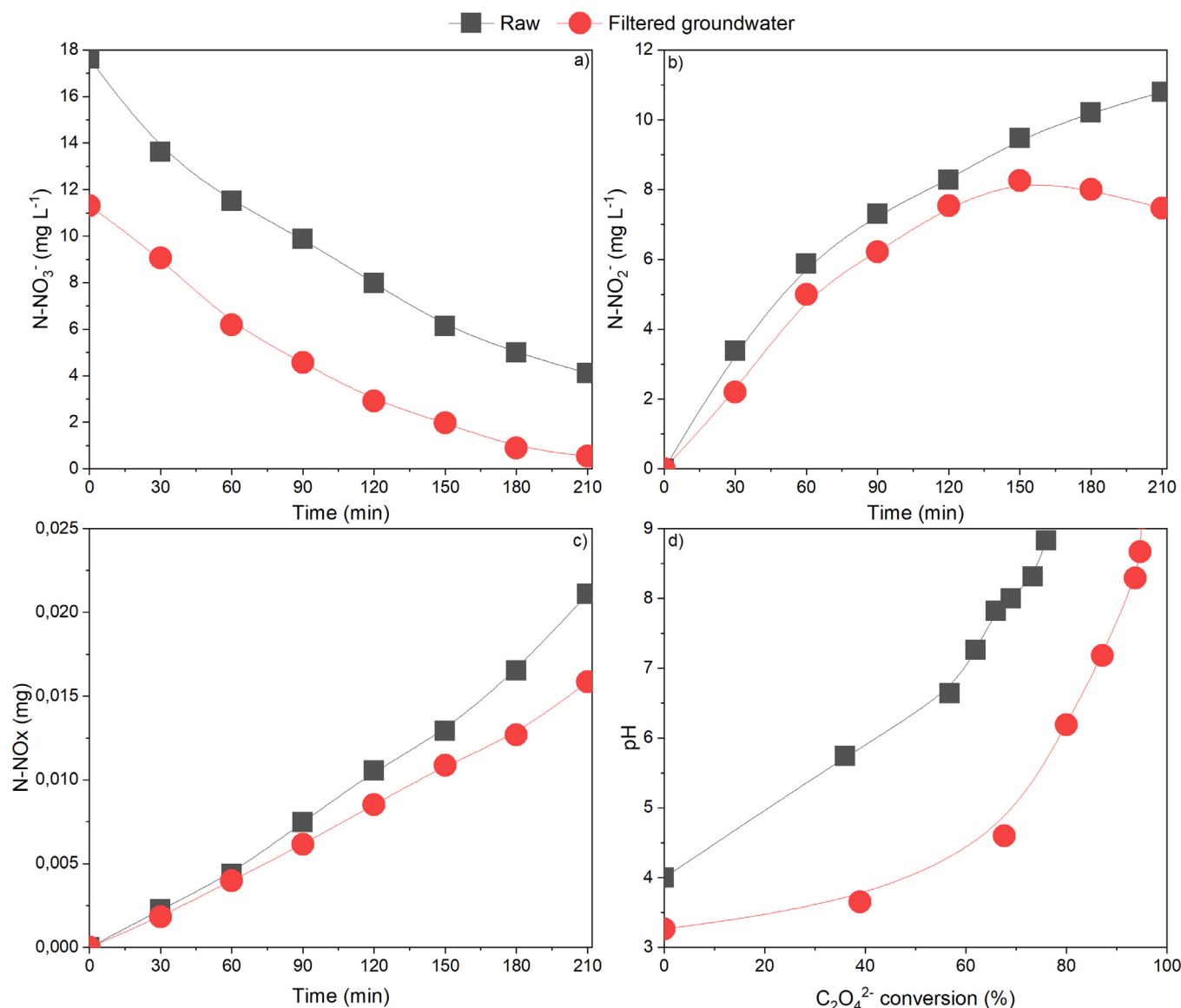
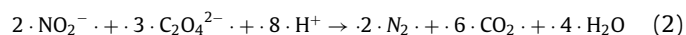
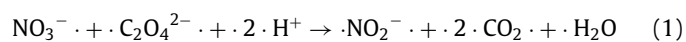


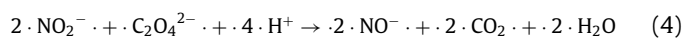
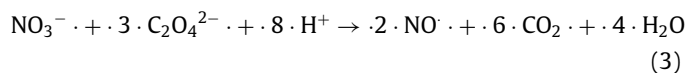
Fig. 1. Experiments using groundwater. Time evolution of NO_3^- photo-reduction. Experimental conditions: $[\text{FeTiO}_3]_0 = 450 \text{ mg/L}$, $[\text{C}_2\text{O}_4^{2-}]_0 = 100\%$, $T = 25^\circ\text{C}$.

The reaction temperature was kept at 25°C by recirculating water (Huber, Germany). Generally, photo-reduction reactions are carried out in an inert atmosphere (N_2) to avoid the competition of dissolved O_2 and NO_3^- for conduction band electrons. Continuous N_2 flow of 370 mL min^{-1} was employed to maintain the reaction system under inert condition.

The $\text{C}_2\text{O}_4^{2-}$ dose was varied between 1 time and 2 times of the stoichiometric value needed for complete reduction of NO_3^- to N_2 , according to Eqs. (1,2).



Besides, both, NO_3^- and NO_2^- could evolve to NO (as a majority NO_x component; see Fig. S3) according to Eqs (3,4).



Experiments to assess the catalytic performance of FeTiO_3 in the presence of typical groundwater ions were performed in deionized water using the stoichiometric $\text{C}_2\text{O}_4^{2-}$ dose and 50 mg/L NO_3^- as starting concentration. Similarly, real groundwater (before and

Table 2
Groundwater samples characterization.

Parameter (mg/L)								
Samples	TC	TOC	TIC	N - NO_3^-	Ca^{2+}	Cl^-	SO_4^{2-}	pH
Raw water (RW)	55.6	5.6	50	17.6	176	15.2	11.3	7.5
Filtered water (TW)	46.4	2.5	43.9	11.3	64	14.7	10.2	6.2

Notes: TC: total carbon; TOC: total organic carbon; TIC: total inorganic carbon.

Table 3

Summary of the experimental outcome achieved in this work. Experimental conditions: $[\text{FeTiO}_3]_0 = 450 \text{ mg/L}$, $[\text{C}_2\text{O}_4^{2-}]_0 = 100\% - 200\%$, $T = 25^\circ\text{C}$.

Selectivity (%) N_2	N-NO_2^- -residual (%)		ϵ	Final pH	Apparent kinetic constant of NO_3^- reduction $k_{\text{app}} \times 10^2 \text{ (min}^{-1}\text{)}$	r^2
Ultrapure water	98.8	0	62.8	7.8	2.78	0.99
Raw water $[\text{C}_2\text{O}_4^{2-}] = 100\%$	15.2	61.2	9.6	8.8	0.69	0.99
Raw water $[\text{C}_2\text{O}_4^{2-}] = 200\%$	83.7	13.7	26.1	7.4	1.52	0.98
Filtered water $[\text{C}_2\text{O}_4^{2-}] = 100\%$	29.1	66.1	18.1	8.5	1.30	0.98
Filtered water $[\text{C}_2\text{O}_4^{2-}] = 200\%$	> 95	0	29.6	5.8	1.44	0.99
HCO_3^- (160 mg/L)	31.6	61.2	19.8	8.8	1.37	0.99
Ca^{2+} (60 mg/L)	83.9	13.4	52.7	8.7	2.54	0.98
K^+ (10 mg/L)	98.8	0	62.1	8.1	2.71	0.97
SO_4^{2-} (90 mg/L)	97.7	0.35	61.4	8.7	2.56	0.98
Cl^- (80 mg/L)	98.3	0.44	61.7	8.8	2.69	0.98
Mg^{2+} (20 mg/L)	94.7	3.2	59.5	7.4	2.54	0.99

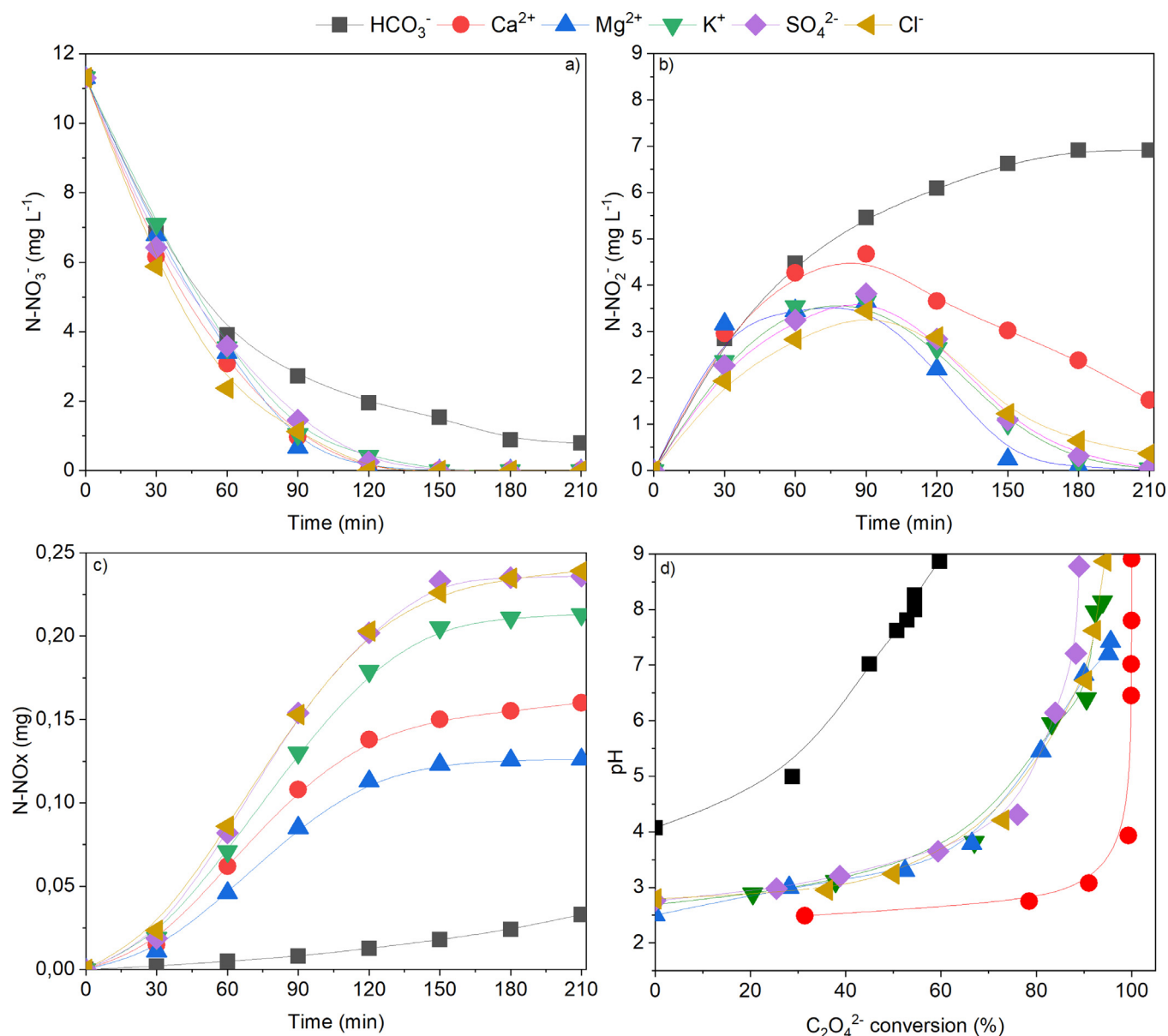


Fig. 2. Experiments using ultrapure water. Effect of isolated ions on NO_3^- photoreduction (a). Evolution of N vs $\text{C}_2\text{O}_4^{2-}$ conversion (b). Experimental conditions: $[\text{FeTiO}_3]_0 = 450 \text{ mg/L}$, $[\text{C}_2\text{O}_4^{2-}]_0 = 100\%$, $[\text{NO}_3^-] = 50 \text{ mg/L}$, $[\text{HCO}_3^-] = 160 \text{ mg/L}$, $[\text{Ca}^{2+}] = 60 \text{ mg/L}$, $[\text{Mg}^{2+}] = 20 \text{ mg/L}$, $[\text{K}^+] = 10 \text{ mg/L}$, $[\text{SO}_4^{2-}] = 90 \text{ mg/L}$, and $[\text{Cl}^-] = 80 \text{ mg/L}$.

after filtration) was used to check natural matrix effects on photocatalytic performance as well the effect of $\text{C}_2\text{O}_4^{2-}$ dose on N_2 selectivity. In all the experiments, FeTiO_3 load was set at 450 mg/L (Fig. S4). Samples withdrawn at regular time intervals were filtered through 0.45 μm Millipore filters and instantly analyzed.

2.4. Analytical methodology

Nitrate, nitrite and oxalic acid were analyzed by ion chromatography (IC) with chemical suppression (Metrohm 790 IC) using a conductivity detector. NO_x concentrations in the gas phase were monitored by a chemiluminescence NO_x analyzer (CLD 63 Eco-physics) and recorded every second. The difference between the initial N concentration and the sum of the N in the identified compounds is attributed to the formation of N_2 . Total Carbon (TC), total organic carbon (TOC), total inorganic carbon (TIC) and total nitrogen (TN) were measured with a TOC-L with TNM analyzer (Shimadzu). Calcium was determined by an atomic absorption spectrophotometer (AA 7000, Shimadzu). Thermogravimetric analyses (TGA) was performed in a thermoscale TGA Q500 (TA Instruments).

3. Results and discussion

The reduction of nitrate was carried out in groundwater before (RW) and after (TW) filtration. RW presented high concentration of calcium, 176 mg/L. The filtration was able to reduce this value to 64 mg/L Ca^{2+} and to eliminate 36% of nitrate and 16% of TC (Table 2). The NO_3^- reduction and the concentrations of NO_2^- , NO_x and $\text{C}_2\text{O}_4^{2-}$ during each treatment (in min) were plotted in Fig. 1. Also, the pH effect on $\text{C}_2\text{O}_4^{2-}$ conversion was included. Due to calcium concentration, both RW and TW turned into a milky solution after adding the hole scavenger $\text{C}_2\text{O}_4^{2-}$, reducing therefore light transmittance through the aqueous medium. Oxalate and calcium cations react yielding insoluble oxalate microcrystals (CaC_2O_4). This was confirmed by TGA analysis (Fig S5) (Bong et al., 2017). Therefore, approximately 60% (RW) and 35% (TW) of $\text{C}_2\text{O}_4^{2-}$ precipitated before the beginning of the photocatalytic reaction.

As shown in Fig. 1a, the initial nitrate reduction rate was almost halved in RW than in TW. In other words, the higher is the salt concentration, the lower is the observed reaction rate. Comparing these results with data obtained using ultrapure water (UW), the reduction rate was approximately four times lower (UW: $2.7 \times 10^{-2} \text{ min}^{-1}$, TW: $1.30 \times 10^{-2} \text{ min}^{-1}$, RW: $0.69 \times 10^{-2} \text{ min}^{-1}$). Nitrate reduction of 76% and 95% after 210 min of reaction were obtained in RW and TW, respectively. While nitrate concentration decays, NO_2^- and NO_x (g) were the first byproducts detected in the aqueous and gaseous phases, respectively (Fig. 1b). Their formation trends indicate that NO_3^- reduction follows two parallel routes. As Fig. 1b shows, NO_2^- formation is the main route while NO_x (g) selectivity was remarkably lower (Fig. 1c). Although the reduction of nitrate to nitrite has been observed, the remaining N-NO_2^- was higher than 60% in both RW and TW.

Approaching the pH influence and as indicated in Eqs. (1–4), this photodegradation process consumes H^+ . Therefore, an acidic pH value foments the reaction. Moreover, this condition also increases the adsorption of the anions NO_3^- and $\text{C}_2\text{O}_4^{2-}$ onto the catalyst surface, which isoelectric point lays around 4.5 (Morin et al., 2017). This justifies the observed higher conversion of $\text{C}_2\text{O}_4^{2-}$ in the pH range of 2.5 to 5. At neutral and basic conditions, the conversion rate decreases (Fig. 1d). To evaluate the treatment efficacy, the yield of $\text{C}_2\text{O}_4^{2-}$ (ϵ) was quantified, as the amount of N (in mg) converted to N_2 by the weight of $\text{C}_2\text{O}_4^{2-}$ (in g) added. Results are gathered in Table 3. This table also summarizes the main outcomes of this research. The maximum theoretical value of ϵ to complete elimination of N, to a stoichiometric dose of $\text{C}_2\text{O}_4^{2-}$ is

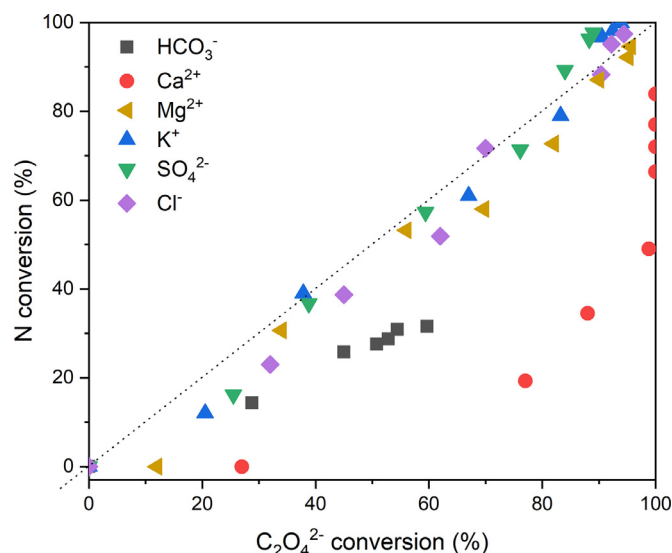


Fig. 3. Evolution of N vs $\text{C}_2\text{O}_4^{2-}$ conversion. Experimental conditions: $[\text{FeTiO}_3]_0 = 450 \text{ mg/L}$, $[\text{C}_2\text{O}_4^{2-}]_0 = 100\%$, $[\text{NO}_3^-] = 50 \text{ mg/L}$, $[\text{HCO}_3^-] = 160 \text{ mg/L}$, $[\text{Ca}^{2+}] = 60 \text{ mg/L}$, $[\text{Mg}^{2+}] = 20 \text{ mg/L}$, $[\text{K}^+] = 10 \text{ mg/L}$, $[\text{SO}_4^{2-}] = 90 \text{ mg/L}$, and $[\text{Cl}^-] = 80 \text{ mg/L}$.

62.83 mg N/ g $\text{C}_2\text{O}_4^{2-}$. Therefore, 29% of this maximum theoretical value (18.27 mg N/ g $\text{C}_2\text{O}_4^{2-}$) was achieved in TW. This yield was about twice the value obtained for RW, 9.64 mg N/ g $\text{C}_2\text{O}_4^{2-}$, being both significantly lower than the value achieved using UW, pointing out the relevancy of the groundwater composition upon the process efficiency. Overall, the selectivity of N_2 was below 30%.

Therefore, a row of experiments was performed to assess the effect of natural groundwater photosensitizers in the photoreduction rate of NO_3^- . Using the average concentration of ions in Spanish groundwater as reference, the influence of bicarbonate (HCO_3^-), calcium (Ca^{2+}), magnesium (Mg^{2+}), potassium (K^+), sulfate (SO_4^{2-}) and chlorite (Cl^-) was investigated (Fig. 2). As shown in Fig. 2, even if the reduction of NO_3^- to NO_2^- took place, the presence of dissolved ions increased the selectivity of NO_2^- in some cases. Analyzing the effect of HCO_3^- , it was observed the decrease of reaction rate (Fig. 2b). Using this ion in solution, the starting pH is acid (4.1) but it increases quickly to alkali (pH = 8.8) through the photoreduction reaction (Fig. 2d).

When pH increases, the ions OH^- compete with species as NO_3^- , NO_2^- and $\text{C}_2\text{O}_4^{2-}$ for the catalytic centers, that adsorb preferentially OH^- . Therefore, followed reaction of NO_2^- to N_2 (Eq. (2)) is stopped. The constant reaction velocity of the electron donors $\text{C}_2\text{O}_4^{2-}$ changed from $0.99 \times 10^{-2} \text{ min}^{-1}$ in the first 60 min of treatment to $0.19 \times 10^{-2} \text{ min}^{-1}$ due to pH increase to values higher than 6. In this condition the oxalate reduction was higher than 60%. The ions NO_2^- may adsorb onto the catalyst surface under acidic conditions, while the adsorbed NO_2^- could desorb at higher pH (Chaplin et al., 2006). In addition, the inhibition effect NO_2^- can be explained by the competition with NO_3^- and HCO_3^- adsorption in the active centers of FeTiO_3 once both ions are structurally similar (Pintar et al., 1998). Consequently, the selectivity to gaseous nitrogen was lower than 35%.

In the case of Ca^{2+} , due to the formation of microcrystals, approximately 27% of oxalate have precipitated before the photocatalytic reaction (Fig. 3), resulting in a remaining high concentration of nitrite and a N_2 selectivity below 85%.

Also, still considering the results with calcium, it was observed a further N conversion once oxalic acid was already no detected in the aqueous phase, probably due to the of calcium oxalate according to its solubility product constant.

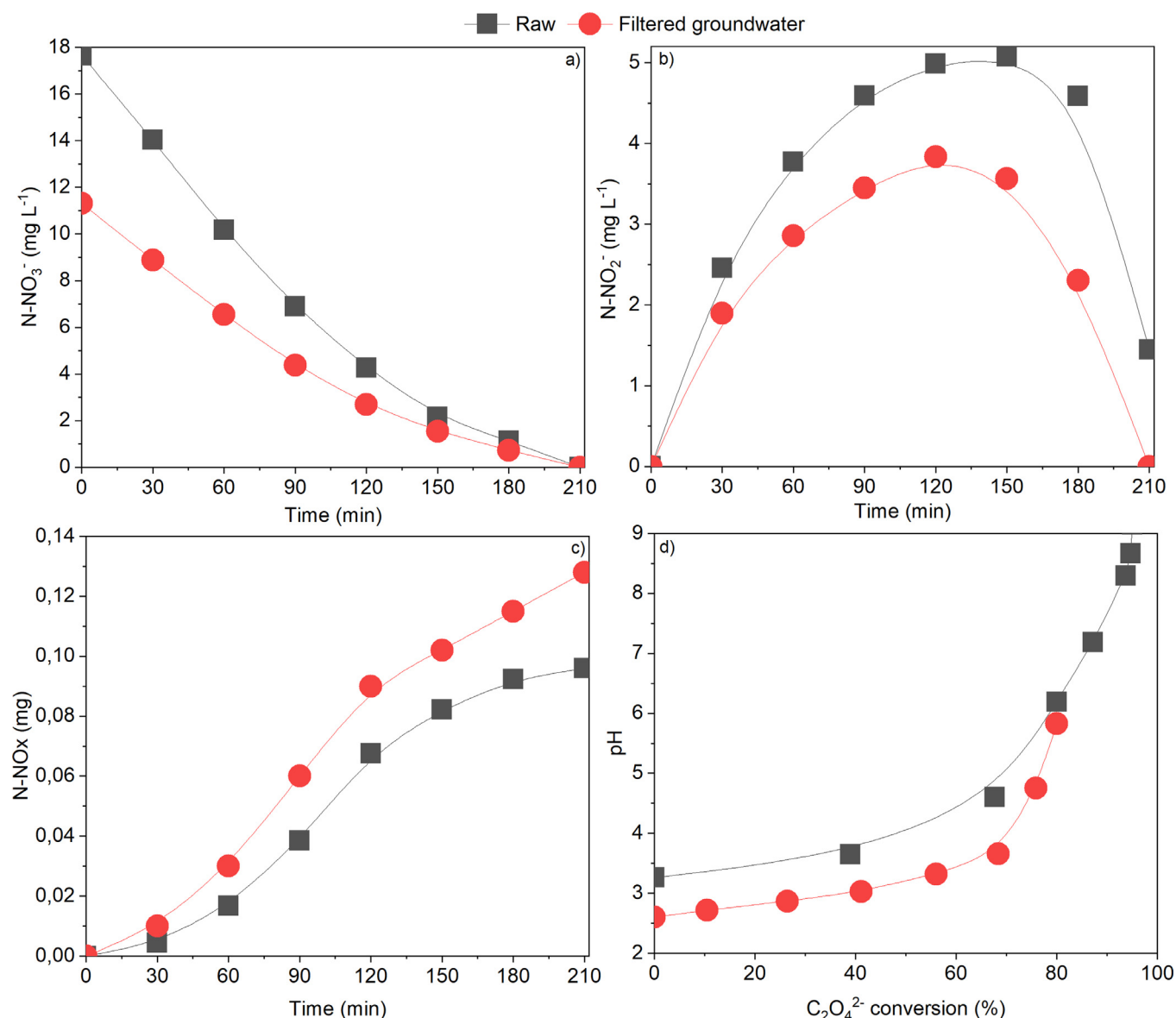


Fig. 4. Experiments using excess of hole scavenger. Time evolution of NO₃⁻ photo-reduction. Experimental conditions: [FeTiO₃]₀ = 450 mg/L, [C₂O₄²⁻]₀ = 200%, T = 25 °C. Raw (black symbol) and filtered water (red symbols).

Oxalic acid when it binds to Mg²⁺ can lead to the formation of MgC₂O₄ microcrystals. Consequently, approximately 12% of C₂O₄²⁻ was precipitated. In fact, this justifies the significant residual N-NO₂⁻ remaining in this experiment (3.2%). The contribution of K⁺, SO₄²⁻ and Cl⁻ (within the studied range) showed a negligible effect in the N₂ selectivity (less than 1.5%). It was demonstrated that the total reduction of nitrate was slower in TW than in RW, due to the presence of solubilized ions mainly Ca²⁺, Mg²⁺ and HCO₃⁻ that both, compete with nitrate for the FeTiO₃ active centers and promote C₂O₄²⁻ precipitation. However, despite a lower efficiency, the use of C₂O₄²⁻ still shows some advantages compared to other well-known hole scavengers, as formic acid, related to its scarce toxicity (Zazo et al., 2007) and the ease to remove the remaining concentration by bubbling air in the system, once TN is totally removed (Zazo et al., 2020).

Fig. 4 portrays the pH effect on the nitrate reduction during the 210 min of reaction in different experimental conditions and using an oxalate stoichiometric dose of 200%. High values of oxalate removal were achieved, but the final pH values here mainly ba-

sic. An exception was the experiment carried out with TW, where the final pH was circumneutral (Fig. 4d). In fact, this justifies the high yield obtained in this experiment. On the other hand, when higher pH values were achieved, the formation of calcium oxalate was increased which hindered the reaction. Considering the reaction using the double stoichiometric dose of oxalic acid, a high total nitrate removal was obtained. The formation of nitrite was also observed and, after 2 h of treatment, the later was converted to N₂, independent of the used matrix. In both RW and TW the highest selectivity to N₂ was achieved, being 92% for RW and 81% for TW, respectively. For RW, a final pH of 7.5 was reached while for TW this value was 5.8. It can be explained by the higher concentration of intact oxalate in the end of this reaction, which may be presented as precipitate material.

Our results indicate that controlling the reactional solution pH is critical. Avoiding its increase, the availability of ions hydroxyl is therefore reduced. It was also exposed that pH control enhances the conversion of nitrate. Indeed, the reduction agent availability showed high importance. It may be exemplified by the higher

degradation rates observed when oxalic acid concentration was inserted in stoichiometric excess (Table 3). On the other hand, lower selectivity to N_2 was obtained when the stoichiometric relation of hole scavenger and NO_3^- was 100%.

Finally, to learn on the stability of the catalyst, three successive runs were carried out using the recovered $FeTiO_3$. It was observed a slightly activity loss due to the possible formation of carbon deposits (Fig. S6) (confirmed by TGA/Derivative Thermogravimetry - DTG analysis), and corrosion promotion (Fig. S7) (confirmed by X-Ray diffraction - XRD analysis) on the ilmenite surface. The selectivity of N_2 dropped gradually to 92 (after 2nd run) and 82% (after 3rd run) (Fig. S8).

$$\varepsilon = \text{mg N converted} / \text{g } C_2O_4^{2-} \text{ fed}$$

4. Conclusion

Natural water matrix constituents can affect the photocatalytic reduction rate of nitrate when the low-cost catalyst ilmenite ($FeTiO_3$) and oxalic acid as electron donor are used. Considering the nitrate contamination of groundwater in Spain as well as in other critical areas, the photocatalytic treatment used in this work appears as a promising alternative. Therefore, the efficacy of the proposed treatment was confirmed in an ideal and unlike condition, where nitrate is a sole aqueous contaminant. To further prove this treatment feasibility, similar experiments were carried out in natural groundwater before and after ultrafiltration. Through these essays, the major controlling factors related to the process yield were identified. In this sense, calcium (Ca^{2+}) and bicarbonate (HCO_3^-) simultaneously present with nitrate, severely affect the selectivity towards N_2 . Also, the reactional pH value can influence the hole scavenger oxalic acid removal, affecting therefore the posterior formation of N_2 .

It was proved that the stoichiometric dose of the reduction agent oxalic acid results in an insufficient nitrate transformation, both in raw and filtered groundwater. Using this 100% proportion, the main byproduct formed is nitrite, which toxicity is well known. Also, in these conditions, the final pH was basic, promoting the formation of calcium oxalate, its precipitation and resulting in the catalyst deactivation. Apart from the almost total conversion of $C_2O_4^{2-}$, in these conditions a low formation of N_2 was achieved. Interestingly, using a dose corresponding to the 200% of the stoichiometric amount of $C_2O_4^{2-}$ required for the reduction of nitrate, N_2 selectivity values of 80% and 95% were obtained respectively for filtered and raw waters. In this case, the matrices composition played an important role in the pH values evolution during the treatment. When raw groundwater was employed, a final pH value of 7.5 was obtained, resulting in an oxalic acid removal of approximately 70% after 210 min of reaction. This hole scavenger reduction promotes a higher selectivity towards N_2 (83.7%). On the other hand, the final pH in the experiments using filtered water was 5.8, resulting therefore in higher conversion of $C_2O_4^{2-}$. Further research at pilot scale will be performed to assess the feasibility of this technology in continuous mode experiments.

Declaration of Competing Interest

None.

Acknowledgments

This work has been supported by AEI (10.13039/501100011033) through the project PID2019-106884GB-I00 and Comunidad de Madrid through the project P2018/EMT-4341. A.R.R thanks the Post-Doctoral scholarship awarded by the public agency São Paulo State Research Foundation (FAPESP), grant #2018/09697-8. J. Carbajo wants to thank the Ministerio de Ciencia, Inno-

vación y Universidades (MICIU) for a grant under the Juan de la Cierva_Incorporación programme (IJCI-2017-32682).

Supplementary materials

Supplementary material associated with this article can be found, in the online version, at doi:10.1016/j.watres.2021.117250.

Reference

- Biddau, R., Cidu, R., Ghiglieri, G., Da Pelo, R., Carletti, A., Pittalis, D., 2017. Nitrate occurrence in groundwater hosted in hard-rock aquifers: estimating background values at a regional scale. *Ital. J. Geosci* 136, 113–124. <https://doi.org/10.1016/j.jgg.2016.03>.
- Bong, W.C., Vanhanen, L.P., Savage, G.P., 2017. Addition of calcium compounds to reduce soluble oxalate in a high oxalate food system. *Food Chem* 221, 54–57. doi:10.1016/j.foodchem.2016.10.031.
- Camargo, J.A., Alonso, A., Salamanca, A., 2005. Nitrate toxicity to aquatic animals: a review with new data for freshwater invertebrates. *Chemosphere* 58, 1255–1267. doi:10.1016/j.chemosphere.2004.10.044.
- Chaplin, B.P., Roundy, E., Guy, K.A., Shapley, J.R., Werth, C.I., 2006. Effects of natural water ions and humic acid on catalytic nitrate reduction kinetics using an alumina supported Pd-Cu catalyst. *Environ. Sci. Technol.* 40, 3075–3081. doi:10.1021/es0525298.
- COM (2018) 257 final. Report from the commission to the council and the European parliament. Brussels, 4.5.2018.
- García-Costa, A.L., Sarabia, A., Zazo, J.A., Casas, J.A., 2020. UV-assisted catalytic wet peroxide oxidation and adsorption as efficient process for arsenic removal in groundwater. *Catal. Today* 1–7. doi:10.1016/j.cattod.2020.03.054.
- García-Muñoz, P., Pliego, G., Zazo, J.A., Bahamonde, A., Casas, J.A., 2016. Ilmenite ($FeTiO_3$) as low cost catalyst for advanced oxidation processes. *J. Environ. Chem. Eng.* 4, 542–548. doi:10.1016/j.jece.2015.11.037.
- Jensen, V.B., Darby, J.L., Seidel, C., Gorman, C., 2014. Nitrate in potable water supplies: alternative management strategies. *Crit. Rev. Environ. Sci. Technol.* 44 (20), 2203–2286. doi:10.1080/10643389.2013.828272.
- Karanasios, K.A., Vasiliadou, I.A., Pavlou, S., Vayenas, D.V., 2010. Hydrogenotrophic denitrification of potable water: a review. *J. Hazard. Mater.* 180, 20–37. doi:10.1016/j.jhazmat.2010.04.090.
- Krempa, H.M., Flickinger, A.K., 2017. Temporal changes in nitrogen and phosphorus concentrations with comparisons to conservation practices and agricultural activities in the Lower Grand River, Missouri and Iowa, and selected watersheds. *Sci. Investig. Rep.* 1969–2015. doi:10.3133/sir20175067.
- Li, X., Wang, S., An, H., Dong, G., Feng, J., Wei, T., Ren, Y., Ma, J., 2021. Enhanced photocatalytic reduction of nitrate enabled by Fe-doped $LiNbO_3$ materials in water: performance and mechanism. *Appl. Surf. Sci.* 539, 148257. doi:10.1016/j.apsusc.2020.148257.
- Liu, X., Huang, M., Bao, S., Tang, W., Fang, T., 2020. Nitrate removal from low carbon-to-nitrogen ratio wastewater by combining iron-based chemical reduction and autotrophic denitrification. *Bioresour. Technol.* 301, 122731. doi:10.1016/j.biortech.2019.122731.
- Mayorga, P., Moyano, A., Anawar, H.M., García-Sánchez, A., 2013. Temporal variation of arsenic and nitrate content in groundwater of the Duero River Basin (Spain). *Phys. Chem. Earth* 58–60, 22–27. doi:10.1016/j.pce.2013.04.001.
- Morín, M.E.Z., Torres-Martínez, L., Sánchez-Martínez, D., Gómez-Solís, C., 2017. Photocatalytic performance of titanates with formula $MTiO_3$ (M= Fe, Ni, and Co) synthesized by solvo-combustion method. *Mater. Res.* 20, 1322–1331. doi:10.1590/1980-5373-MR-2016-0615.
- Pennino, M.J., Compton, J.E., Leibowitz, S.G., 2017. Trends in drinking water nitrate violations across the United States. *Environ. Sci. Technol.* 51, 13450–13460. doi:10.1021/acs.est.7b04269.
- Pintar, A., Šetinc, M., Levec, J., 1998. Hardness and salt effects on catalytic hydrogenation of aqueous nitrate solutions. *J. Catal.* 174, 72–87. doi:10.1006/jcat.1997.1960.
- Ruiz-Beviá, F., Fernández-Torres, M.J., 2019. Effective catalytic removal of nitrates from drinking water: an unresolved problem? *J. Clean. Prod.* 217, 398–408. doi:10.1016/j.jclepro.2019.01.261.
- Silveira, J.E., Paz, W.S., García-Muñoz, P., Zazo, J.A., Casas, J.A., 2017. UV-LED/ilmenite/persulfate for azo dye mineralization: the role of sulfate in the catalyst deactivation. *Appl. Catal. B Environ.* 219, 314–321. doi:10.1016/j.apcatb.2017.07.072.
- SWD (2018) 246 final. Commission Staff Working Document. Part 1/9. Brussels, 4.5.2019.COM (2018) 257 final. Report from the commission to the council and the European parliament. Brussels, 4.5.2018.
- Unión Europea. (2006). Directiva 2006/118/CE del Parlamento Europeo y del Consejo relativa a la protección de las aguas subterráneas contra la contaminación y el deterioro. 27 de Diciembre de 2006, 2006, 1–13.
- Velu, M., Balasubramanian, B., Velmurugan, P., Kamyab, H., Ravi, V.A., Chelliapan, S., Lee, C.T., Palaniyappan, J., 2021. Fabrication of nanocomposites mediated from aluminium nanoparticles/Moringa oleifera gum active carbon for effective photocatalytic removal of nitrate and phosphate in aqueous solution. *J. Clean Prod.* 281, 124553. doi:10.1016/j.jclepro.2020.124553.
- Wang, L., Fu, W., Zhuge, Y., Wang, J., Yao, F., Zhong, W., Ge, X., 2021. Synthesis of polyoxometalates (POM)/ TiO_2 /Cu and removal of nitrate nitrogen in water by photocatalysis. *Chemosphere* 278, 130298.

- W.H.O (World Health Organization), 2011. **Nitrate and Nitrite in Drinking Water. Background Document for Development of WHO Guidelines for Drinking Water Quality.** WHO/SDE/WSH/07.01/16/Rev/1, Geneva, p. 31.
- Yang, T., Doudrick, K., Westerhoff, P., 2013. Photocatalytic reduction of nitrate using titanium dioxide for regeneration of ion exchange brine. *Water Res.* 47, 1299–1307. doi:[10.1016/j.watres.2012.11.047](https://doi.org/10.1016/j.watres.2012.11.047).
- Zazo, J.A., García-Muñoz, P., Pliego, G., Silveira, J.E., Jaffe, P., Casas, J.A., 2020. Selective reduction of nitrate to N₂ using ilmenite as a low cost photo-catalyst. *Appl. Catal. B Environ.* 273, 1–6. doi:[10.1016/j.apcatb.2020.118930](https://doi.org/10.1016/j.apcatb.2020.118930).
- Zazo, J.A., Casas, J.A., Molina, C.B., Quintanilla, A., Rodriguez, J.J., 2007. Evolution of ecotoxicity upon fenton's oxidation of phenol in water. *Environ. Sci. Technol.* 41, 7164–7170. doi:[10.1021/es071063l](https://doi.org/10.1021/es071063l).
- Zhang, F., Jin, R., Chen, J., Shao, C., Gao, W., Li, L., Guan, N., 2005. High photocatalytic activity and selectivity for nitrogen in nitrate reduction on Ag/TiO₂ catalyst with fine silver clusters. *J. Catal.* 232, 424–431. doi:[10.1016/j.jcat.2005.04.014](https://doi.org/10.1016/j.jcat.2005.04.014).